Journal of the Indian Chemical Society 99 (2022) 100400

Contents lists available at ScienceDirect

Journal of the Indian Chemical Society

journal homepage: www.journals.elsevier.com/journal-of-the-indian-chemical-society

Spectroscopic (FTIR, UV-Vis, NMR) investigations, DFT predictions of global reactivity descriptors and efficient corrosion inhibitors of *N*-carbobenzoxy-L-ValineSuccinimidyl Ester

D. Devi [a,b], M.M. Armstrong Arasu [b,*], A. Mary Girija [a,b]

[a] PG & Research Department of Physics, Cauvery College for Women, Autonomous, Tiruchirappalli, 620018, TN, India
[b] Department of Physics, St. Joseph's College, Autonomous, Affiliated to Bharathidasan University, Tiruchirappalli, 620002, TN, India

ARTICLE INFO

Keywords:
DFT
FT-IR
NMR
N-Carbobenzoxy-L-Valine-Succinimidyl Ester
Global reactivity descriptors
Corrosion inhibitors

ABSTRACT

The stable conformation of molecular structure, vibrational frequencies and electronic absorption spectra of *N*-Carbobenzoxy-L-Valine-Succinimidyl Ester were established using DFT/B3LYP/6-311G basis set calculations. The compound was characterized by spectroscopic profiling employing FT-IR, UV–Visible and NMR spectra both experimentally and theoretically. The HOMO–LUMO analysis was carried out with different applied electric fields. Molecular Electrostatic Potential (MEP), First order hyperpolarizability, and Fukui functions calculation were also performed. The global reactivity descriptors were calculated to establish the relationship between the descriptors and corrosion inhibition efficiency. Molecular orbital calculations reveal that the molecule may be bioactive based on its global reactivity.

1. Introduction

An amino acid is a biomolecule with vital importance to all living organisms. These biomolecules form proteins and many essential substances, such as neurotransmitters, hormones, and nucleic acids [1]. These molecules are considered in several scientific research studies related to nutrition, drug delivery and plant protection. The term amino acid is used to describe molecules containing both amino (–NH2) and carboxyl (–COOH) groups. The carboxylic acid group offers its proton to the amino group. Hence, in a solid state, amino acids exist as zwitterion.

The branched-chain structure of L-Valine is a decisive factor in the properties of the amino acids. The side chains in amino acids have a powerful inductive effect on reactivity. Basically, amino acids that possess both amino groups and acidic carboxyl groups have many properties and are highly reactive [2]. Since amino acids are readily biodegradable and possess high reactivity, adding additional groups to the side chains can add more properties in terms of reactivity to the amino acid. Recently, amino acids have been examined as corrosion inhibitors owing to their high reactivity and biodegradability [3,4]. Corrosion inhibitors are substances that preserve metals by preventing or reducing the corrosion process. Amino acids and their complexes form a family of organic materials with applications in NLO [5,6].

An analysis of the literature shows that neither a quantum chemical study nor an experimental spectroscopic study has been conducted on the molecules which is very important for studying the micro level properties of organic compounds. Since *N*-Carbobenzoxy-L-Valine Succinimidyl Ester (CVSE) is a bioactive material, the results of this density functional theory investigation will contribute to a reliable and profound understanding of possible intramolecular interactions and bioactivity of the compound under study. The research into their derivatives has attracted considerable interest from both theoretical and synthetic organic chemists for progress towards developing biologically active compounds useful in chemistry, biology and medicine.

Therefore, in the present study, the molecular structure of CVSE is studied with the density functional theory (B3LYP/6-311G) methods. In addition, this study focuses on a broad description of isotropic chemical shifts, excitation energy and HOMO–LUMO energies of CVSE. The global reactivity descriptors, namely, ionization potential (I.P), hardness (η), chemical potential (μ), electron affinity (E.A), softness (s), electronegativity (χ), electrophilicity index (ω), electronic charge transfer (ΔN), nucleofugality (ΔEn), electrofugality (ΔEe), $\Delta E_{back\text{-}donation}$ are also calculated to realize the reactive nature of the compound. Besides, the dipole moment, and first order hyperpolarizability are also studied using the DFT/B3LYP employing the 6-311G basis set. Additionally, this study also highlights the geometrical and electronic structure, electrostatic potential surfaces, and vibrational spectra of (CVSE) based on

* Corresponding author.
E-mail address: armstrongarasu@gmail.com (M.M.A. Arasu).

https://doi.org/10.1016/j.jics.2022.100400
Received 8 December 2021; Received in revised form 19 February 2022; Accepted 23 February 2022
Available online 26 February 2022

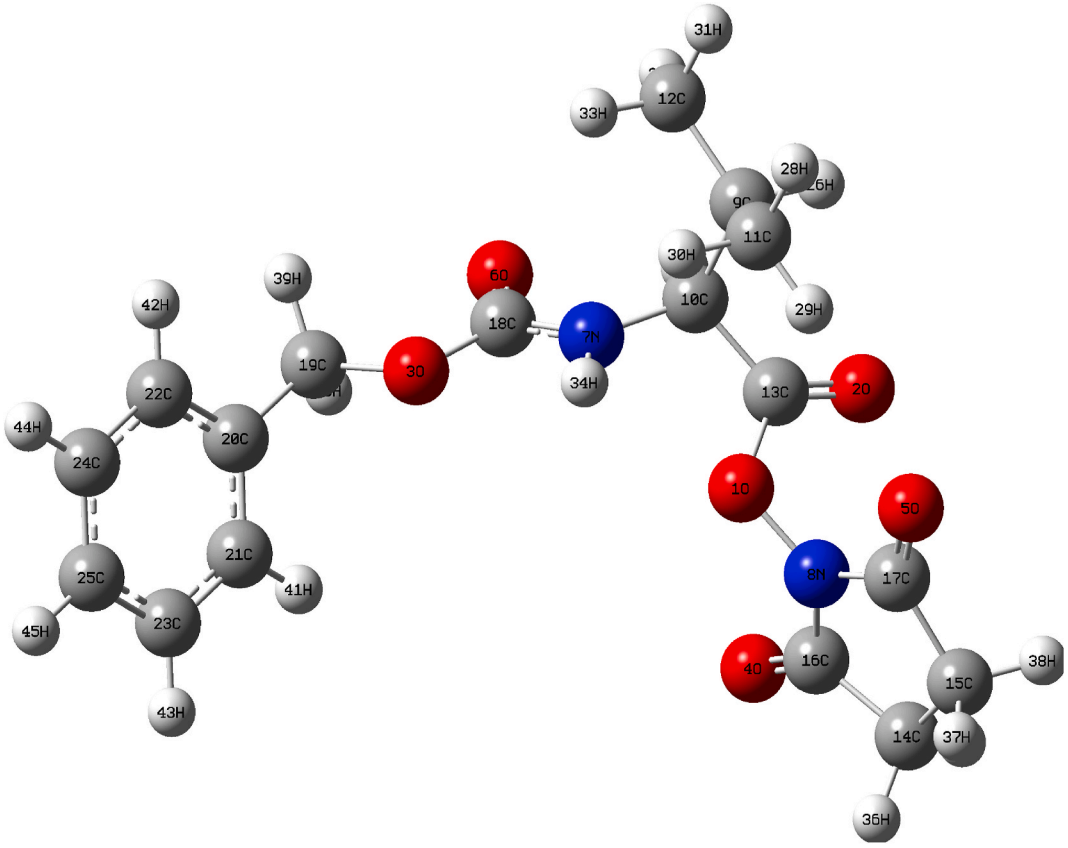

Fig. 1. Optimized structure of carbobenzoxy-L-valinesuccinimidyl Ester.

experimental spectral analysis and density functional theory (DFT) computations. Based on these theoretically calculated descriptors, the corrosion inhibition properties of the title compound were evaluated.

2. Experimental details

The compound under investigation namely *N*-Carbobenzoxy-L-Valine Succinimidyl Ester (CVSE) was purchased from TCI chemicals. FT-IR spectra of the compound were recorded in a PERKIN ELMER spectrometer, in the range of 4000–400 cm-1. The spectral resolution is ±2 cm^{-1}. The UV-Vis spectrum in water solvent was recorded by employing the Lambda-365 PerkinElmer spectrophotometer as part of the spectral range of 1100-190 nm. In order to record the ^{13}C NMR and ^{1}H NMR spectra of the CVSE molecule, the Bruker 400 MHz Avance FT-NMR spectrometer was used, with TMS as an internal standard (Fig. 6), using deuterated chloroform ($CDCL_3$) as the solvent.

3. Computational details

The primary task in the computational study is to determine the optimized geometry of the compound (CVSE). A DFT-B3LYP/6-311G simulation was used to check on the structural characteristics and the vibrational modes using the GAUSSIAN 09W [6] program. Based on the same level of theory, the HOMO-LUMO, frequency, TD-DFT and NMR have been analyzed.

4. Results and discussions

4.1. Molecular geometry

The optimized molecular structure of CVSE is shown in Fig. 1 and Table 1 summarizes the comparative structural parameters, including bond lengths, bond angles, and dihedral angles. Most of the calculated bond lengths are higher in the theoretical calculations than in the experimental results because the theoretical calculations encompass an isolated molecule in a gaseous phase, whereas experimental results encompass a molecule in a solid state [7]. According to the calculated values of B3LYP/6-311G, the order of the bond length is as C21–C23 < C24–C25 < C22–C24< C20–C22 < C20–C21< C19–C20< C10–C13 < C15–C17 < C14–C16 < C9–C12 < C9–C11< C14–C15 < C9–C10. From the order of bond length, it is evident that the ring symmetry is distorted and particularly they are more elongated in the substitution place in the structure of CVSE. The bond length of N8–O1 (1.4042A°). All the calculated bond length of the ring C–H are greater than the experimental value (1.001A°) [8]. The bond length between C7 and N10 is 0.0337°A times smaller than the experimental value (1.487A°) [9] when compared with B3LYP/6-311G basis set. According to the experimental value [10], the bond angle of C16–N8–O1 and C17–N8–O1 are 121.8955° and 121.4597° which are 1.7045° and 2.1403° differed from the calculated values by B3LYP/6-311G.

4.2. Vibrational spectral analysis

The band assignment of complex molecules was successfully performed by vibrational spectroscopy coupled with quantum mechanical calculations [11]. It is the most useful experimental technique for the study of hydrogen-bonded complexes. The aim of the vibrational analysis is to discover the vibrational modes associated with specific molecular structures of the title compound. CVSE consists of 45 atoms. The experimental FT-IR spectrum is shown in Fig. 2. The observed and calculated frequencies are presented in Table 2.

Molecularly, Valine has two methyl groups in the side chain. The vibrations of CH3 stretching and deformation are more or less localized, and give rise to good group wavenumbers. The C–H stretching vibrations

Table 1
Optimized Parameters of *N*-Carbobenzoxy-L-Valine Succinimidyl Ester using B3LYP/6-311G method.

Bond Length	Values (Å)	Exp[a]	Bond Angle	Values (Å)	Exp[a]	Dihedral Angle	Values (Å)
O1–N8	1.4042	–	N8–O1–C13	113.0704	–	C13–O1–N8–C16	−93.4233
O1–C13	1.4399	1.469	C18–O3–C19	116.2569	–	C13–O1–N8–C17	86.5592
O2–C13	1.215	1.292	C10–N7–C18	121.3927	121.0	N8–O1–C13–O2	1.2479
O3–C18	1.3819	1.341	C10–N7–H34	120.2751	119.4	N8–O1–C13–C10	−175.6494
O3–C19	1.4874	1.469	C18–N7–H34	117.7848	119.4	C19–O3–C18–O6	1.1963
O4–C16	1.2262	1.232	O1–N8–C16	121.8955	123.6	C19–O3–C18–N7	−179.1336
O5–C17	1.2293	1.232	O1–N8–C17	121.4597	123.6	C18–O3–C19–C20	169.6937
O6–C18	1.2416	1.247	C16–N8–C17	116.6447	121.0	C18–O3–C19–H39	−69.1665
N7–C10	1.4533	1.487	C10–C9–C11	112.2814	111.8	C18–O3–C19–H40	48.0646
N7–C18	1.3645	1.336	C10–C9–C12	109.875	110.1	C18–N7–C10–C9	114.7331
N7–H34	1.0059	0.910	C10–C9–H26	105.4455	107.6	C18–N7–C10–C13	−119.8069
N8–C16	1.4051	1.336	C11–C9–C12	111.7375	111.8	C18–N7–C10–H27	−3.6391
N8–C17	1.4002	1.336	C11–C9–H26	108.5825	108.0	H34–N7–C10–C9	−73.9401
C9–C10	1.5685	1.535	C12–C9–H26	108.6574	108.0	H34–N7–C10–C13	51.5199
C9–C11	1.5383	1.535	N7–C10–C9	113.7223	110.1	H34–N7–C10–H27	167.6877
C9–C12	1.5365	1.535	N7–C10–C13	113.1737	110.1	C10–N7–C18–O3	176.7106
C9–H26	1.0942	1.230	N7–C10–H27	106.327	108.0	C10–N7–C18–O6	−3.6248
C10–C13	1.5119	1.518	C9–C10–C13	109.2657	110.1	H34–N7–C18–O3	5.1754
C10–H27	1.0915	0.981	C9–C10–H27	107.7225	108.0	H34–N7–C18–O6	−175.16
C11–H28	1.0913	1.001	C13–C10–H27	106.1674	107.6	O1–N8–C16–C4	1.5978
C11–H29	1.0914	1.001	C9–C11–H28	109.8665	108.0	O1–N8–C16–C14	−178.4222
C11–H30	1.0929	1.001	C9–C11–H29	112.6764	–	C17–N8–C16–C4	−178.3855
C12–H31	1.0915	1.001	C9–C11–H30	110.9581	111.2	C17–N8–C16–C14	1.5945
C12–H32	1.0912	1.001	H28–C11–H29	107.5786	108.2	O1–N8–C17–O5	−1.8184
C12–H33	1.0915	1.001	H28–C11–H30	107.2456	–	O1–N8–C17–C15	178.2737
C14–C15	1.5478	1.539	H29–C11–H30	108.3102	108.2	C16–N8–C17–O5	178.165
C14–C16	1.5201	1.520	C9–C12–H31	110.013	–	C16–N8–C17–C15	−1.743
C14–H35	1.0892	1.001	C9–C12–H32	111.6966	–	C11–C9–C10–N7	60.7518
C14–H36	1.0895	1.001	C9–C12–H33	110.9062	–	C11–C9–C10–C13	−66.7604
C15–C17	1.5185	1.518	H31–C12–H32	108.2016	108.2	C11–C9–C10–H27	178.3193
C15–H37	1.0896	1.001	H31–C12–H33	107.8998	108.2	C12–C9–C10–N7	−64.2579
C15–H38	1.0892	1.001	H32–C12–H33	107.9974	108.2	C12–C9–C10–C13	168.2299
C19–C20	1.5001	1.505	O1–C13–O2	121.8416	125.9	C12–C9–C10–H27	53.3096
C19–H39	1.0889	1.001	O1–C13–C10	111.0532	–	H26–C9–C10–N7	178.8187
C19–H40	1.0885	1.001	O2–C13–C10	127.0218	122.7	H26–C9–C10–C13	51.3064
C20–C21	1.4028	–	C15–C14–C16	106.1283	–	H26–C9–C10–H27	−63.6138
C20–C22	1.4009	–	C15–C14–H35	112.7339	109.9	C10–C9–C11–H28	177.2076
C21–C23	1.3952	–	C15–C14–H36	112.9232	109.9	C10–C9–C11–H29	57.2736
C21–H41	1.0825	1.001(3)	C16–C14–H35	108.6594	108.0	C10–C9–C11–H30	−64.3705
C22–C24	1.3972	–	C16–C14–H36	108.9891	108.0	C12–C9–C11–H18	−58.8126
C22–H42	1.0829	–	H35–C14–H36	107.3012	–	C12–C9–C11–H29	−178.7467
C23–C25	1.3987	–	C14–C15–C17	105.948	–	C12–C9–C11–H30	59.6092
C23–H43	1.0819	1.001(3)	C14–C15–H37	112.9301	–	H26–C9–C11–H28	61.0145
C24–C25	1.3967	–	C14–C15–H38	112.8212	–	H26–C9–C11–H29	−58.9196
C24–H44	1.0819	1.001(3)	C17–C15–H37	109.0207	–	H26–C9–C11–H30	179.4363
C25–H45	1.0819	0.990(3)	C17–C15–H38	108.7229	–	C10–C9–C12–H31	−175.8548
			H37–C15–H38	107.2945	108.2	C10–C9–C12–H32	−55.676
			O4–C16–N8	125.3911	123.6	C10–C9–C12–H33	64.8515
			O4–C16–C14	129.1372	–	C11–C9–C12–H31	58.8234
			N8–C16–C14	105.4717	–	C11–C9–C12–H32	179.0022
			O5–C17–N8	125.1736	123.6	C11–C9–C12–H33	−60.4703
			O5–C17–C15	129.045		H26–C9–C12–H31	−60.9597
			N8–C17–C15	105.7813	107.0	H26–C9–C12–H32	59.2191
			O3–C18–O6	124.3491	123.6	H26–C9–C12–H33	179.7466
			O3–C18–N7	109.9577	–	N7–C10–C13–O1	−16.8275
			O6–C18–N7	125.6923	123.6	N7–C10–C13–O2	166.474
			O3–C19–C20	107.4567	–	C9–C10–C13–O1	110.9929
			O3–C19–H39	108.1367	–	C9–C10–C13–O2	−65.7055
			O3–C19–H40	107.7986	–	H27–C10–C13–O1	−133.0898
			C20–C19–H39	112.0503	–	H27–C10–C13–O2	50.2118
			C20–C19–H40	112.6205	–	C16–C14–C15–C17	−0.2231
			H39–C19–H40	108.5953	108.2	C16–C14–C15–H37	119.0469
			C19–C20–C21	120.3655	–	C16–C14–C15–H38	−119.0681
			C19–C20–C22	120.6564	–	H35–C14–C15–C17	118.6105
			C21–C20–C22	118.9732	–	H35–C14–C15–H37	−122.1195
			C20–C21–C23	120.5493	–	H35–C14–C15–H38	−0.2345
			C20–C21–H41	119.4457	–	H36–C14–C15–C17	−119.5671
			C23–C21–H41	120.0047	–	H36–C14–C15–H37	−0.2971
			C20–C22–C24	120.617	–	H36–C14–C15–H38	121.588
			C20–C22–H42	119.4879	–	C15–C14–C16–O4	179.251
			C24–C22–H42	119.895	–	C15–C14–C16–O8	−0.728
			C21–C23–C25	120.0535	–	H35–C14–C16–O4	57.7674
			C21–C23–H43	119.8954	–	H35–C14–C16–N8	−122.2116
			C25–C23–H43	120.0508	–	H36–C14–C16–O4	−58.8585

(*continued on next page*)

Table 1 (*continued*)

Bond Length	Values (Å)	Exp[a]	Bond Angle	Values (Å)	Exp[a]	Dihedral Angle	Values (Å)
			C22–C24–C25	119.9823	–	H36–C14–C16–N8	121.1625
			C22–C24–H44	119.9068	–	C14–C15–C17–O5	−178.8077
			C25–C24–H44	120.1109	–	C14–C15–C17–N8	1.0954
			C23–C25–C24	119.8238	–	H37–C15–C17–O5	59.3814
			C23–C25–H45	120.075	–	H37–C15–C17–N8	−120.7154
			C24–C25–H45	120.1011	–	H38–C15–C17–O5	−57.2892
						H38–C15–C17–N8	122.6139
						O3–C19–C20–C21	−78.1328
						O3–C19–C20–C22	101.0485
						H39–C19–C20–C21	163.2184
						H39–C19–C20–C22	−17.6003
						H40–C19–C20–C21	40.4329
						H40–C19–C20–C22	−140.3858
						C19–C20–C21–C23	179.3605
						C19–C20–C21–H41	−0.4619
						C22–C20–C21–C23	0.1656
						C22–C20–C21–H41	−179.6569
						C19–C20–C22–C24	−179.534
						C19–C20–C22–H42	0.4542
						C21–C20–C22–C24	−0.3415
						C21–C20–C22–H42	179.6467
						C20–C21–C23–C25	0.0721
						C20–C21–C23–H43	179.8931
						H41–C21–C23–C25	179.8936
						H41–C21–C23–H43	−0.2854
						C20–C22–C24–C25	0.2794
						C20–C22–C24–H44	−179.7658
						H42–C22–C24–C25	−179.7087
						H42–C22–C24–H44	0.2461
						C21–C23–C25–C24	−0.1372
						C21–C23–C25–H45	179.7675
						H43–C23–C25–C24	−179.958
						H43–C23–C25–H45	−0.0532
						C22–C24–C25–C23	−0.0372
						C22–C24–C25–H45	−179.942
						H44–C24–C25–C23	−179.992
						H44–C24–C25–H45	0.1033

[a] REF [8.9.10].

are among the most stable in the spectrum. The stretching vibrations of the CH_3 and C–H group amino acid complexes are assigned as a number of sharp bands in the region 2980–2875 cm^1 [12–15]. The observed medium band at 2965 cm^{-1} is assigned for asymmetrical stretching of methyl 2. The medium band at 2876 cm^{-1} is assigned for the asymmetrical stretching of methyl 1. The IR bands at 1463 cm^{-1} (strong) and 1421 cm^{-1} (medium) are attributed to the in-plane bending vibrations of Methyl 1&2. These bands occur because two distinct CH3 groups are present in the amino acid residues. Out of plane vibrations of methyl groups occur at 917 & 898 cm^{-1}. The C–H stretching vibrations are naturally established in the range of 3100-3000 cm^{-1} [16,17]. For CVSE it is observed at 3038 cm^{-1}. The in-plane bending modes of C–H are observed between 1300 and 1000 cm^{-1}. The peak at 1530 cm^{-1} is attributed to CVSE's aromatic C–H in-plane bending vibration. The C–H out-of-plane bending modes of benzene derivatives are seen in the range 1000–600 cm^{-1}. The C–H out of plane bending modes of CVSE are seen at 698 cm^{-1}. The ring carbon–carbon stretching modes lie in the range from 1650 to 1200 cm^{-1} [13]. C–C stretching vibrations are observed at 1354 and 1312 cm^{-1} respectively. C–C in-plane and out of plane bending vibrations of CVSE are occurred at 753 and 465 cm^{-1} respectively.

In the IR spectra, the stretching vibration of C═O causes characteristic bands, and this intensity can be increased by hydrogen bond formation or conjugation. The carbonyl compounds give rise to strong bands in the region 1730–1680 cm^{-1} [9]. For CVSE, C═O stretching modes are observed as a medium band at 1782, 1738 &1719 cm^{-1}.

The C–O stretching usually found in the region 1260–1000 cm^{-1} [12]. The peak at 1237 & 1204 cm^{-1} are identified as a C–O stretching vibration of CVSE. The peaks observed at 646 cm^{-1} in the IR spectrum are recognized as C–O in-plane bending vibration for CVSE.

In CVSE, the stretching vibration of N–H appears at 3362 cm^{-1}. The in-plane bending peak is identified at 1635 cm^{-1} and the frequency observed at 812 cm^{-1} was assigned as N–H out-of-plane bending mode of CVSE. All vibrations are agreed well with the literature. The C–N stretching mode is allotted to the wave numbers observed at 1072 and 1022 cm^{-1} in the FT-IR spectrum.

4.3. UV-Vis Spectral analysis

Calculations in gas phase and solvents were performed using TD-DFT/B3LYP/6-311G method to gain a greater insight into electronic transitions of CVSE. The calculated absorption wavelengths (λ), oscillator strengths (f), and excitation energies (E) are given in Table 3. The experimental and theoretical UV-Vis spectrum of CVSE is shown in Fig. 3 (a and b) for gas phase and solvents.

The absorption maxima for CVSE was found at 251.29 nm for gas phase and 231.84 nm, 232.47 nm for aniline and chloroform respectively. Absorption peak shows a significant blue-shifted absorption wavelength relatively. This absorbance maxima is due to possibility of n-π* transition which involves the transfer of electron from non-bonded atomic orbitals along with carbonyl O-atom to the first molecular excited state of CVSE. On the basis of the calculated absorption spectrum, the highest absorption wavelength corresponds to the electronic transition from HOMO-2 → LUMO+1, which contributes 81% to the gaseous absorption spectrum and from the HOMO-2 → LUMO for the non-polar solvents, which contributes 78%.The HOMO-2→LUMO+1 transition with 87% contribution in DMSO. This HOMO to LUMO transition confirms the electron density transfer. In light of this photophysical property, the electron density may be concentrated on an electron-donor, i.e. the radical responsible for sensitizing the photo-to-

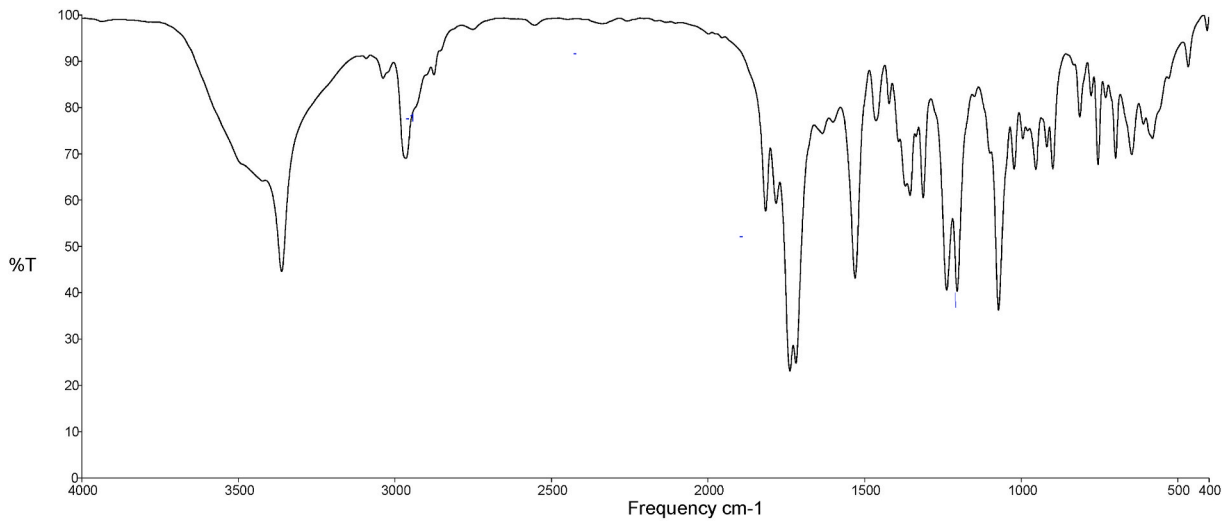

(a)

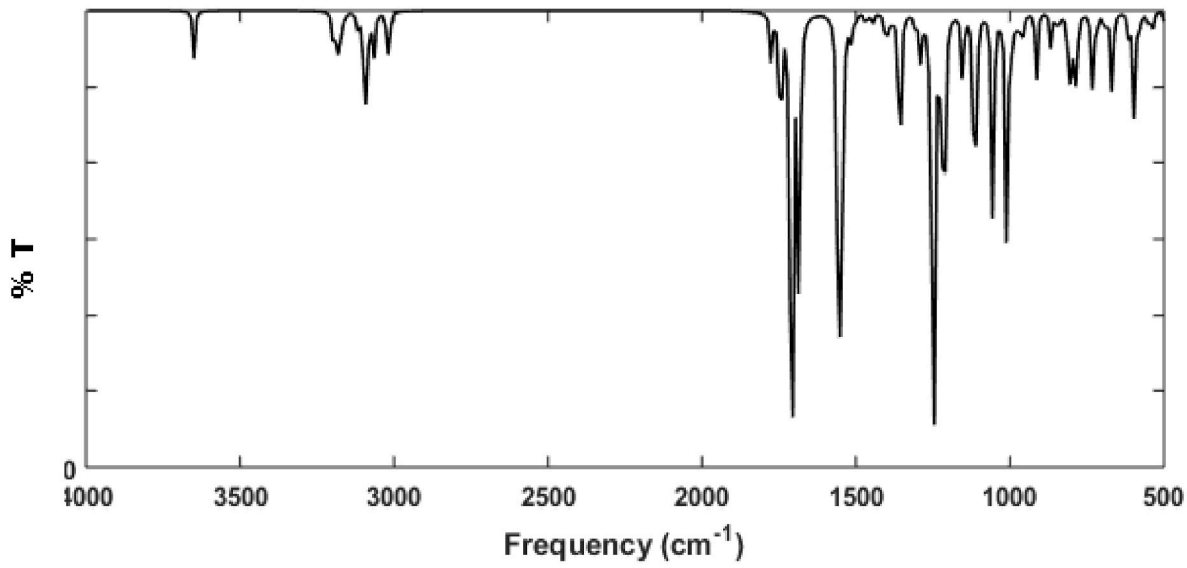

(b)

Fig. 2. (a) Experimental and (b) theoretical IR spectra of Carbobenzoxy-L-Valine succinimidyl Ester.

current conversion process. Polar solvents improves the probability of these transitions and inturn enrich the charge transfer process.

4.4. Impact of electric fields on HOMO–LUMO analysis

HOMO (ability of electron giving) and LUMO (ability of electron accepting) are the core orbitals taking part in every chemical reaction. A molecule's kinetic stability, chemical reactivity, optical polarizability, chemical hardness and softness can be determined by its energy gap [16]. A few important molecular orbitals (MO) were examined for CVSE as shown in Fig 4a and Fig 4b. These are the surfaces for frontier orbitals that define the CVSE bonding scheme. The positive segment is red and the negative one is green. figure (4) clearly shows that the HOMOs are mostly localized on the ring, while the LUMOs are mainly confined to the nitro group and ring.

HOMO energy = −8.3096eV
LUMO energy = −4.1021eV
HOMO–LUMO gap = 4.2075eV

The HOMO–LUMO analysis is made at B3LYP/6–311G level for the electric field such as 0, 0.005, 0.01 and 0.015 VA^{-1}. Fig. 4 visualizes the spreading of HOMO over the ring carbons and the oxygen of CVSE for zero field. Here LUMOs are concentrated on the succinimide group. By increasing the field (0.005–0.015 VA^{-1}) the HOMO–LUMO gap reduces from 4.2075 eV to 0.1425 eV for *N*-Carbobenzoxy-L- Valine Succinimidyl ester (CVSE) (as shown in Table 5). This large decrease in gap is stating the possibility of having sensible conduction through the molecule; subsequently, the conductivity increases due to a reduction in energy gap [17].

Table 2
Vibrational assignments of wavenumbers for *N*-Carbobenzoxy-L-Valine Succinimidyl Ester along with the theoretical wavenumbers at (B3LYP/6-311G) level.

S. No.	Experimental FT-IR wavenumbers (cm^{-1})	Theoretical wavenumbers (cm^{-1})	Assignments
1.	3362	3198	υNH
2.	3038	3023	υCH
3.	2965	3021	υasCH3
4.	2876	3014	υasCH3
5.	1782	1776	υC = O
6.	1738	1746	υC = O
7.	1719	1709	υC = O
8.	1635	1650	δNH
9.	1601	1627	υNO
10.	1530	1528	δCH
11.	1463	1467	δCH3
12.	1421	1424	δCH3
13.	1354	1355	υCC
14.	1312	1306	υCC
15.	1237	1227	υCO
16.	1204	1209	υCO
17.	1072	1058	υCN
18.	1022	1030	υCN
19.	994	991	δ_C = O
20.	953	963	δ_C = O
21.	917	914	γCH3
22.	898	877	γCH3
23.	812	808	γNH waging
24.	776	783	υC-C-C
25.	753	734	δCC
26.	729	729	δCN
27.	698	692	γCH waging
28.	646	653	δCO
29.	609	615	γC = O
30.	579	578	γC = O
31.	465	495	γCC
32.	405	415	δC-C-C

υ_s, υ_{as}: symmetric–asymmetric stretching,; δ in-plane bending,; γ out-of-plane bending.

4.5. Global reactivity descriptors

Chemical potential is defined by the first-order partial derivatives of total energy (E) with respect to the number of electrons (N) at constant external potential v(r) and global hardness (η) is defined by the second-order partial derivatives of total energy (E) with respect to the number of electrons (N) at constant external potential v(r) [18].

$$\mu = -\chi = \left(\frac{\partial E}{\partial N}\right)_{V(r)} \tag{1}$$

$$\eta = \frac{1}{2}\left(\frac{\partial^2 E}{\partial N^2}\right)_{V(r)} = \frac{1}{2}\left(\frac{\partial \mu}{\partial N}\right)_{V(r)} \tag{2}$$

Calculation of chemical hardness based on I.P and E.A is,

$$\eta \approx \frac{I.P - E.A}{2} \tag{3}$$

Using Koopman's theorem [18] for closed-shell compounds, S & μ can be defined as

$$S = \frac{1}{\eta} \tag{4}$$

$$\mu = \frac{-(I.P + E.A)}{2} \tag{5}$$

Here, I.P and E.A are the ionization potential and electron affinity of the compounds respectively. As the electron affinity of a ligand is defined by its capability to accept electrons from a donor, the ionization energy of atoms and molecules is a measure of their chemical reactivity. High ionization energy indicates a high level of stability as well as chemical inertness. Molecular stability and reactivity can be assessed by the absolute hardness of a compound and its absolute softness [19].

Another qualitative measurement is the electrophilicity index (ω), which defines the quantitative nature of a compound's electrophilicity [20]. It is a measure of energy lowering due to maximal electron flow between donor and acceptor. The defined electrophilicity index (ω) is given by

$$\omega = \frac{\mu^2}{2\eta} = \frac{\chi^2}{2\eta} \tag{6}$$

The calculated electrophilicity index measure describes the biological activity of CVSE and is used to understand the toxicity of pollutants based on reactivity and site selectivity All calculated values of hardness,

Table 3
Calculated absorption wavelength λ (nm), excitation energies E (eV) and oscillator strengths (f) of *N*-Carbobenzoxy-L-Valine-Succinimidyl Ester calculated using TD-DFT/B3LYP/6-311G basis set.

Parameters	Gas Phase	Polar		Non Polar	
		Aniline	DMSO	Chloroform	CCl_4
Wavelength λ (nm)	251.29	231.84	251.43	232.47	234.44
Excitation energies E(eV)	4.9340	5.3478	4.9312	5.3334	5.2884
Oscillator strengths (f)	0.0076	0.0098	0.0067	0.0090	0.0088
Major contribution	H-2→L+1 (81.16%)	H-2→L (66.94%)	H-2→L+1 (87.12%)	H-2→L (70.05%)	H-2→L (78.88%)

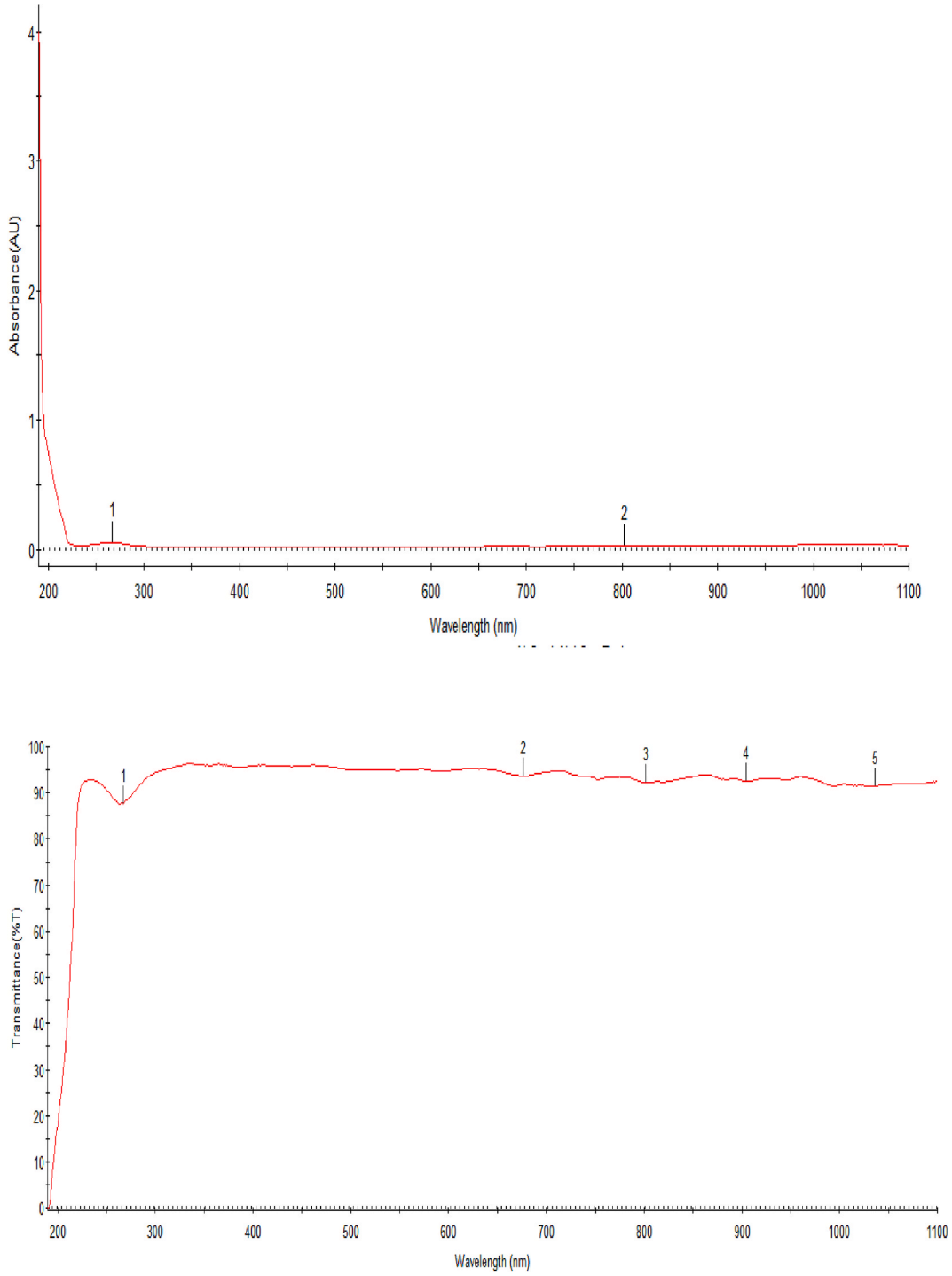

Fig. 3a. Experimental UV-Vis spectra of Carbobenzoxy-L-Valine succinimidyl Ester.

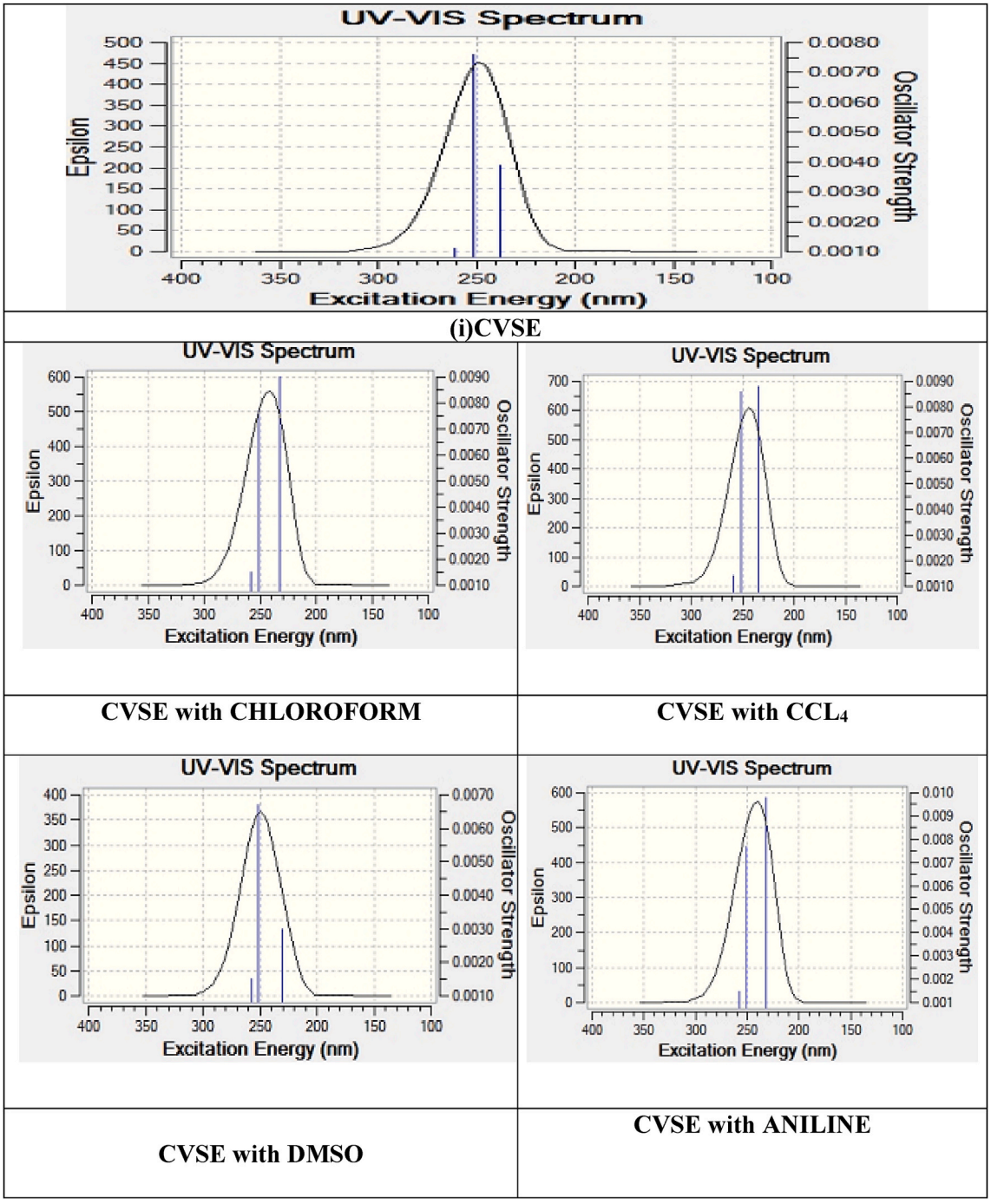

Fig. 3b. Theoretical UV-Vis spectra of Carbobenzoxy-L-Valine succinimidyl Ester.

potential and electrophilicity index are summarized in Table 4. From this table it can be seen that the electric field increases the electrophilicity index. The maximum amount of electronic charge that an electrophilic system can hold is given by the following equation [21].

$$\Delta N = \frac{\chi_{Fe} - \chi_{Inh}}{2(\eta_{Fe} + \eta_{Inh})} \tag{7}$$

where $^{\chi}_{Fe}$ and $^{\chi}_{Inh}$ denote the absolute electronegativity of iron and inhibitor molecule respectively. $^{\eta}_{Fe\ and}$ $^{\eta}_{Inh}$ denote the absolute hardness of iron and the inhibitor molecule respectively. Theoretical value of $^{\chi}_{Fe} =$ 6.38775eV and $^{\eta}_{Fe} = 0$ for the computation of number of transferred electrons. The difference in electronegativity drives the electron transfer (ΔN), and the sum of the hardness parameters acts as a resistance.

$$\Delta E_{back-donation} = -\frac{\eta}{4} \tag{8}$$

The nucleophilic and electrophilic capabilities of leaving group are nucleofugality (ΔE_n) and electrofugality (ΔE_e) and they are defined as follows

$$\Delta E_n = E.A + \omega = \frac{(\mu + \eta)^2}{2\eta} \tag{9}$$

$$\Delta E_n = E.A + \omega = \frac{(\mu - \eta)^2}{2\eta} \tag{10}$$

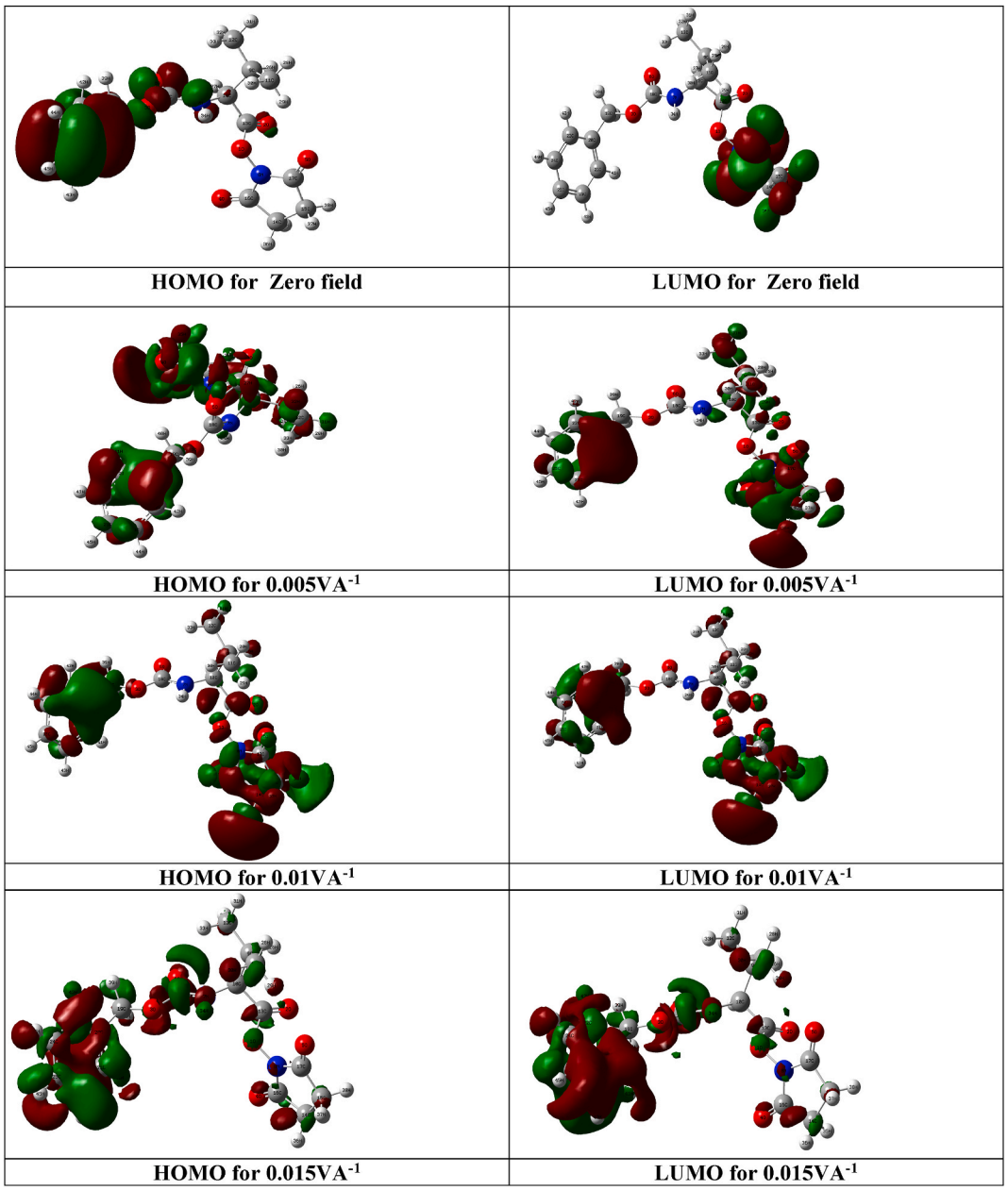

Fig. 4a. HOMO and LUMO of Carbobenzoxy-L-Valine-Succinimidyl Ester for various applied electric field.

4.5.1. Chemical hardness

Chemical hardness is a useful measure for assessing the behaviour of chemical systems. It determines how resistant a group of nuclei and electrons is to changes in its electron distribution [19]. As from Table (4), the chemical hardness of CVSE is high in gas phase (2.103776 eV) and it is reduced to 0.07128 eV at the applied electric field of 0.015 VÅ^{-1}.

4.5.2. Chemical potential (μ)

Chemical potential (μ) refers to an equilibrium system's inclination for electrons to escape. The values of μ for various applied electric fields are computed using equation (5) and are shown in Table 5. The greater electronic chemical potential leads to lesser stability and more reactivity. As from Table (5), it is evident that CVSE is less stable at 0.015 VÅ^{-1} and thus more reactive. CVSE has the best stability in the gas phase.

4.5.3. Electrophilicity index (ω)

It measures the affinity of the species to accept electrons. A better reactive nucleophile has a lower value of ω, and reversibly higher ω indicates a good electrophile. The value of ω for CVSE increases from 9.153381 to 185.1274 by the applied electric field of 0.015 VÅ^{-1}. Hence this can be employed as a superior electrophile comparatively.

4.6. First hyperpolarizability and dipole moment

The dipole moment and first hyperpolarizability (β) are defined as

$$\mu = \left(\mu_x^2 + \mu_y^2 + \mu_z^2\right)^{1/2} \tag{11}$$

$$\beta = \left(\beta_x^2 + \beta_y^2 + \beta_z^2\right)^{1/2} \tag{12}$$

where, $\beta_x = (\beta_{xxx} + \beta_{xyy} + \beta_{xzz})$

Fig. 4b. DOS of Carbobenzoxy L-Valine Succinimidyl Ester for (a) zero field (b) 0.005 VÅ^{-1} (c) 0.01 VÅ^{-1} (d) 0.015 VÅ^{-1}.

Table 5
The theoretical HOMO energy, LUMO energy, Energy gap (Eg) and Ionization potential (IP), Electron affinity (EA), Hardness (η), Softness (s), Chemical potential (μ), Electronegativity (χ), Electrophilicity index (ω), Charge transfer (ΔNmax), Nucleofugality (ΔEn) and Electrofugality (ΔEe) of *N*-Carbobenzoxy-L-Valine-Succinimidyl Ester by using B3LYP/6-311G for different electric field.

Parameters	Gas Phase (0 VÅ^{-1})	Electric field in VÅ^{-1} (0.005)	Electric field in VÅ^{-1} (0.01)	Electric field in VÅ^{-1} (0.015)
HOMO energy (eV)	−8.3096	−7.7949	−6.4474	−5.2085
LUMO energy(eV)	−4.1021	−4.3176	−5.2429	−5.0660
Energy gap (Eg) (eV)	4.2075	3.4773	1.2045	**0.1425**
Ionization potential (IP)	8.3096	7.7949	6.4474	5.2085
Electron affinity (EA)(eV)	4.1021	4.3176	5.2429	5.0660
Hardness (Ƞ)(eV)	2.1037	1.7386	0.6022	0.0712
Softness (S)(eV)	0.4753	0.5751	1.6604	14.0291
Chemical Potential (μ)	−6.2059	−6.0563	−5.8452	−5.1372
Electronegativity (λ)	6.2059	6.0563	5.8451	5.1372
Electrophilicity index (w)(eV)	9.1533	10.5480	28.3653	185.127
Charge Transfer (ΔN_{max})	2.9498	3.4833	9.7055	72.0719
Nucleofugality (ΔE_n)(eV)	3.9993	5.3610	22.8212	180.0258
Electrofugality (ΔE_e)(eV)	16.4111	17.4736	34.5116	190.3004

$$\beta_y = (\beta_{yyy} + \beta_{xxy} + \beta_{yzz})$$

$$\beta_z = \beta_{zzz} + \beta_{xxz} + \beta_{yyz}$$

Based on the DFT/B3LYP/6-311G method, the dipole moment and first hyperpolarizabilities for CVSE are 3.9395 Debye and 1.9686 × 10^{-30} esu, respectively as shown in Table 6. Urea is one of the classic molecules used for studying the NLO properties of the chemical systems. Therefore, it is primarily used as a threshold for comparative purpose. Computed values of total dipole moment of CVSE is approximately three times greater than those of urea and the first hyperpolarizability of title compound is 5.2 times greater than that of urea (μ and β of urea are 1.3732 Debye and 0.3728 × 10^{-30} esu by 6-311G method). First hyperpolarizability is strongly dependent on the extent of the electronic communication and the complete overlap of orbitals to facilitate the charge transfer from donor to acceptor. The present study reveals that the selected compound have large first static hyperpolarizabilities and may have potential applications in the development of NLO materials.

4.7. Analysis of fukui indices

Electron population around the atoms in a molecule is much useful to investigate the stability of the molecule. The Mullikan population analysis gives, (N − 1), (N) and (N + 1) for all atoms of CVSE. By Yang and Mortier procedure, calculated f_k values in a finite difference approximation [22] is,

$f_k^n = q(N+1) - q(N)$ for nucleophilic attack.

$f_k^e = q(N) - q(N-1)$ for electrophilic attack.

$f_k^r = \frac{1}{2}[q(N+1) - q(N-1)]$ for radical attack or dual descriptor.

Softness indices providing a method to compare the reactivity of similar atoms in different molecules. These indices can be calculated from the relationship between the Fukui function f(k) and the local softness S(k).

The local softness is given by,

$$S(k) = f(k)S$$

$$S^+ = f_k^n S$$

$$S^- = f_k^e S$$

The optimization of CVSE was performed at three different charge states, i.e., neutral, singly positively and negatively charged. The Fukui functions f_k^n and f_k^e points out regions at which the molecule is most able to accommodate the addition and removal of an electron, respectively. Hence, large values of f_k^n, will point out the area which is most susceptible to nucleophilic attacks, while large values of f_k^e will be coupled with regions susceptible to electrophilic attacks.

A molecule's atomic site with the highest condensed Fukui function is more reactive, as Lee et al. [23] determined from their study that the more reactive atomic site during a chemical reaction has the highest

Table 6
Theoretical first hyperpolarizability of *N*-Carbobenzoxy-L-Valine Succinimidyl Esterusing B3LYP/6-311G method.

Parameters	Values for *N*-Carbobenzoxy-L-Valine Succinimidyl Ester(amu)
β_{xxx}	49.1822
β_{xxy}	31.9973
β_{xyy}	93.5094
β_{yyy}	−73.3472
β_{xxz}	−15.7831
β_{yyz}	−71.8746
β_{xzz}	54.4317
β_{yzz}	−53.0352
β_{zzz}	23.1496
β	1.9686 × 10^{-30} esu

Table 4
The theoretical HOMO energy, LUMO energy, Energy gap (Eg) and Ionization potential (IP), Electron affinity (EA), Hardness (η), Softness(s), Chemical potential (μ), Electronegativity (χ), Electrophilicity index (ω), Charge transfer (ΔNmax), Nucleofugality (ΔEn) and Electrofugality (ΔEe) of *N*-Carbobenzoxy-L-Valine-Succinimidyl Ester by using B3LYP/6-311G.

Parameters	Gas Phase	Polar				Non Polar		
		WATER	DMSO	ETHANOL	ANILINE	CCL_4	CHLOROFORM	THF
HOMO energy (eV)	−8.3096	−8.2814	−8.2821	−8.2838	−8.2894	−8.3022	−8.2918	−8.289
LUMO energy (eV)	−4.1021	−4.1140	−4.1138	−4.1137	−4.1125	−4.1103	−4.1119	−4.1127
Energy gap (Eg) (eV)	4.2075	4.1673	4.1682	4.17013	4.1768	4.1919	4.1799	4.1763
Ionization potential (IP) (eV)	8.3096	8.2814	8.2821	8.2838	8.2894	8.3022	8.2918	8.2890
Electron affinity (EA) (eV)	4.1021	4.1140	4.1138	4.1137	4.1125	4.1102	4.1119	4.1127
Hardness (Ƞ) (eV)	2.1037	2.0836	2.0841	2.0850	2.0884	2.0959	2.0899	2.0881
Softness (S) (eV)	0.4753	0.4799	0.4798	0.4796	0.4788	0.4771	0.4784	0.4788
Chemical Potential (μ) (eV)	−6.205	−6.1977	−6.1980	−6.1987	−6.2010	−6.2062	−6.2018	−6.2009
Electronegativity (χ) (eV)	6.2059	6.1977	6.1980	6.1987	6.2010	6.2062	6.2018	6.2009
Electrophilicity index (w) (eV)	9.1533	9.2172	9.2161	9.2143	9.2060	9.1885	9.2018	9.2068
Charge Transfer (ΔN_{max}) (eV)	2.9498	2.9743	2.9739	2.9729	2.9692	2.9610	2.9674	2.9695
Nucleofugality (ΔE_n) (eV)	3.9993	4.0613	4.0602	4.0580	4.0492	4.0302	4.0449	4.0500
Electrofugality (ΔE_e) (eV)	16.4118	16.4567	16.4562	16.4556	16.4513	16.4427	16.4487	16.4518

Table 7
The calculated Fukui indices for *N*-Carbobenzoxy-L-Valine-Succinimidyl Ester using DFT/B3LYP/6-311G method.

ATOMS	q_N	q_{N+1}	q_{n-1}	fe-	fe+	f^r_k	S^+	S^-
O 1	−0.3449	−0.4629	−0.3545	0.0096	−0.1180	−0.0541	−0.0560	0.0045
O 2	−0.3330	−0.4075	−0.2827	−0.0502	−0.0744	−0.0623	−0.0354	−0.0238
O 3	−0.4964	−0.5072	−0.4819	−0.0144	−0.0108	−0.0126	−0.0051	−0.0068
O 4	−0.3282	−0.4036	−0.3702	0.0419	−0.0753	−0.0167	−0.0358	0.0199
O 5	−0.3403	−0.3876	−0.3093	−0.0310	−0.0473	−0.0391	−0.0224	−0.0147
O 6	−0.4320	−0.4673	−0.3738	−0.0582	−0.0352	−0.0467	−0.0167	−0.0276
N 7	−0.6396	−0.6086	−0.5953	−0.0443	0.0310	−0.0066	0.0147	−0.0210
N 8	−0.39614	−0.3190	−0.3971	0.0009	0.0771	0.0390	0.0366	0.0004
C 9	−0.2004	−0.1869	−0.2233	0.0229	0.0134	0.0182	0.0064	0.0109
C 10	−0.1651	−0.1740	−0.1861	0.0209	−0.0088	0.0060	−0.0041	0.0099
C 11	−0.5335	−0.5067	−0.5283	−0.0051	0.0267	0.0107	0.0127	−0.0024
C 12	−0.503831	−0.4962	−0.4965	−0.0073	0.0075	0.0001	0.0035	−0.0034
C 13	0.5831	0.3511	0.5926	−0.0094	−0.2319	−0.1207	−0.1102	−0.0045
C 14	−0.5116	−0.5061	−0.5146	0.0029	0.0054	0.0042	0.0025	0.0014
C 15	−0.5081	−0.5067	−0.5037	−0.0044	0.0013	−0.0015	0.0006	−0.0021
C 16	0.5904	0.5646	0.6124	−0.0220	−0.025	−0.0239	−0.0122	−0.0104
C 17	0.5952	0.5590	0.6035	−0.0082	−0.0362	−0.0222	−0.0172	−0.0039
C 18	0.7146	0.6821	0.7190	−0.0044	−0.0324	−0.0184	−0.0154	−0.0021
C 19	−0.2096	−0.2027	−0.2536	0.0439	0.0069	0.0254	0.0033	0.0209
C 20	0.0040	−0.0382	0.0362	−0.0322	−0.0422	−0.0372	−0.0200	−0.0153
C 21	−0.0916	−0.0975	−0.0533	−0.0383	−0.0058	−0.0221	−0.0027	−0.0182
C 22	−0.1181	−0.1220	−0.0792	−0.0389	−0.0038	−0.0213	−0.0018	−0.0185
C 23	−0.1624	−0.2083	−0.1611	−0.0013	−0.0458	−0.0235	−0.0217	−0.0006
C 24	−0.1624	−0.1767	−0.1340	−0.0284	−0.0142	−0.0213	−0.0067	−0.0135
C 25	−0.1285	−0.1274	−0.0606	−0.0678	0.0010	−0.0334	0.0005	−0.0322
H 26	0.2030	0.1720	0.2258	−0.0227	−0.0310	−0.0268	−0.0147	−0.0108
H 27	0.2682	0.2102	0.2816	−0.0134	−0.0579	−0.0357	−0.0275	−0.0064
H 28	0.1835	0.1311	0.2129	−0.0293	−0.0524	−0.0409	−0.0249	−0.0139
H 29	0.2182	0.2335	0.2199	−0.0016	0.0152	0.0068	0.0072	−0.0007
H 30	0.1706	0.1592	0.1664	0.0041	−0.0113	−0.0035	−0.0053	0.0019
H 31	0.1794	0.1441	0.2078	−0.0284	−0.0352	−0.0318	−0.0167	−0.0135
H 32	0.1884	0.1620	0.1945	−0.0060	−0.0264	−0.0162	−0.0125	−0.0028
H 33	0.1866	0.1771	0.1850	0.0015	−0.0095	−0.0039	−0.0045	0.0007
H 34	0.3624	0.3931	0.3816	−0.0192	0.0307	0.0057	0.01459	−0.0091
H 35	0.2455	0.2027	0.2625	−0.0169	−0.0427	−0.0298	−0.0203	−0.0080
H 36	0.2408	0.1968	0.2538	−0.0129	−0.0440	−0.0284	−0.0209	−0.0061
H 37	0.2413	0.1941	0.2615	−0.0201	−0.0471	−0.0336	−0.0224	−0.0095
H 38	0.2453	0.2062	0.2680	−0.0226	−0.0391	−0.0309	−0.0186	−0.0107
H 39	0.1956	0.1794	0.2530	−0.0573	−0.0162	−0.0367	−0.0077	−0.0272
H 40	0.2099	0.2192	0.2935	−0.0835	0.0092	−0.0371	0.0044	−0.0397
H 41	0.1632	0.2513	0.2486	−0.0854	0.0880	0.0013	0.0418	−0.0406
H 42	0.1582	0.13018	0 .2176	−0.0593	−0.0281	−0.0437	−0.0133	−0.0282
H 43	0.1530	0.14612	0.2226	−0.0695	−0.0069	−0.0382	−0.0033	−0.0330
H 44	0.1517	0.12257	0.2176	−0.0658	−0.0292	−0.0475	−0.0138	−0.0312
H 45	0.1533	0.12548	0.2208	−0.0675	−0.0278	−0.0476	−0.0132	−0.0320

condensed Fukui function value. Sign of dual descriptors can distinguish between nucleophilic and electrophilic attack on a specific site [24]. Table 7 indicates that there is a significant difference in the charge among the atoms. Taking into account the distribution of charges, it appears that H41 is the favored active site for reactions with nucleophilic species, C19 for reactions with electrophiles, N8 for reactions with radical.

4.8. Electrostatic potential analysis

Electrostatic potential (ESP) provides a visible illustration of the chemically active sites and therefore the reactivity of the atoms. The electrostatic potential field caused by a molecular system is known to be closely associated with many of its properties and thus contains valuable information for their description. A low (red) and high (blue) electrostatic potential indicates the electron rich and electron deficient regions, respectively.

ESP surfaces for zero and various electric fields in Fig. 5 shows the charge distribution of CVSE. Here, the positive ESP is identified by the blue region, whereas the red region represents negative ESP [25]. The strong positive contribution is acknowledged from the carboxylic group and the mild positive ESP is established in the vicinity of oxygen atom in *N*-Carbobenzoxy-L-valine succinimidyl ester. This development is almost remaining the same up to the field of 0.015 VÅ^{-1}. Negative ESP is seen over the oxygen atom in the succinimide group and spreads near nitrogen atoms while increasing the field, therefore the electrophilic attack is taking place at nitrogen atoms.

4.9. NMR spectral investigations

Spectral analysis by nuclear magnetic resonance (NMR) can be used to determine the structure of organic compounds. The observed ^{1}H and ^{13}C NMR spectra are provided in Fig. 6a and b, respectively. The ^{1}H and ^{13}C theoretical and experimental chemical shifts, isotropic shielding constants and the assignments are summarized in Tables 8a and Tables 8b. Aromatic carbons give signals with chemical shift values from 100 to 200 ppm [26–28]. The experimental chemical shifts of ring carbons atoms (C20–C25) lie in the range of 134.82–127.36 ppm for CVSE. The presence of partially positive charge on the carbon atoms C13 and C18 in the downfield chemical shift positions of 182.50, 163.11 ppm reveals the presence of carbons that have a partially positive charge. When comparing ring carbons with methyl carbons, C12 appears at 14.00 ppm (theoretically) due to the electron donating effect of methyl groups.

^{1}H chemical shifts were found by complete examination of the NMR spectrum to compute the possible different effects acting over the

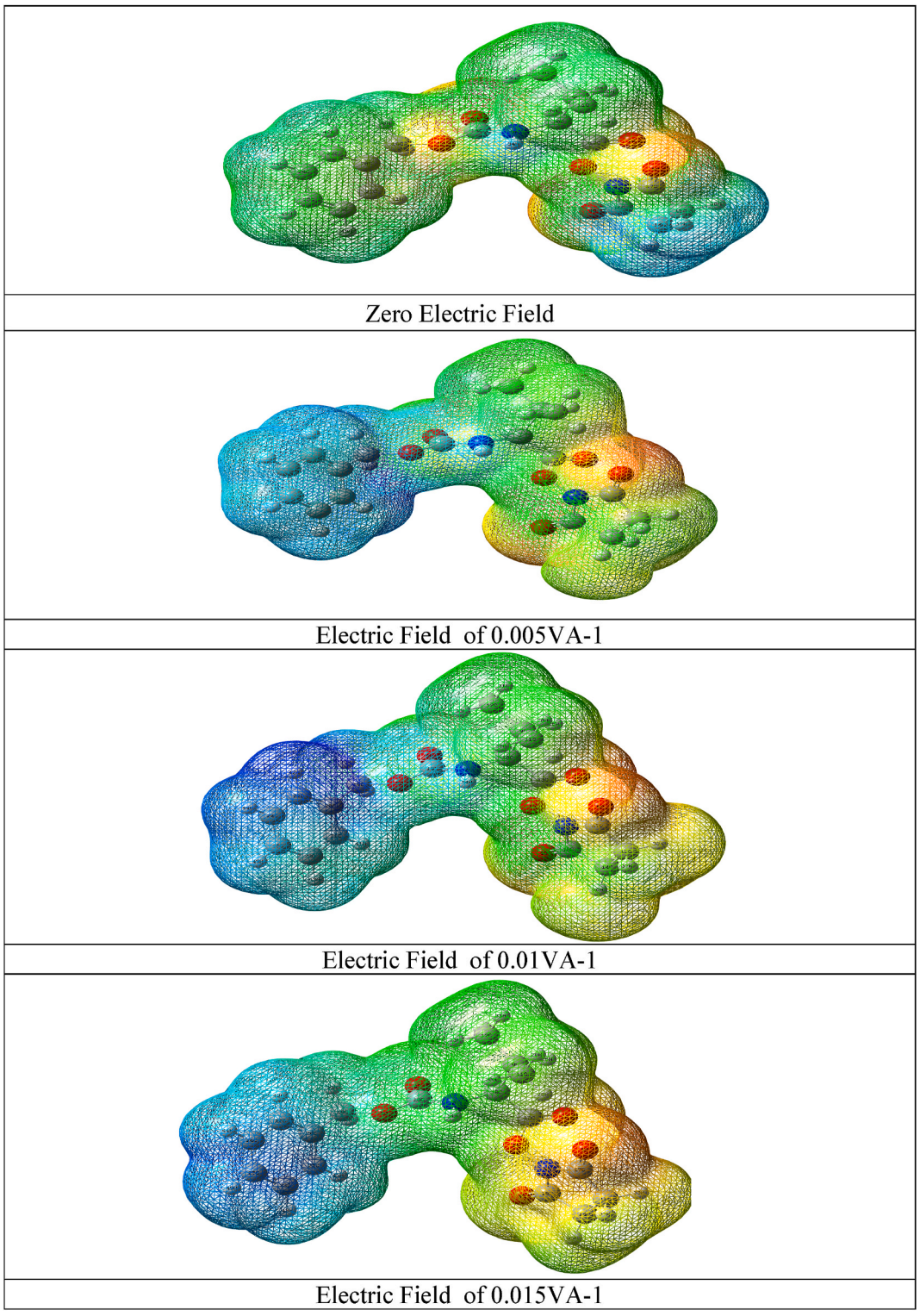

Fig. 5. ESP image of carbobenzoxy L-Valine succinimidyl Ester.

shielding constant of protons. Benzene rings hydrogen have NMR peaks at 6.60–6.47 ppm for while C-methylene hydrogen atoms are observed at 1.962–4.406 ppm, and *N*-hydrogen atoms show peak at 3.99 ppm, which indicates that these protons are under high magnetic shielding.

4.10. Corrosion inhibitor efficiency analysis

Metals (including iron and copper) can be effectively and economically protected from corrosion by using corrosion inhibitors [29]. Organic compounds containing oxygen, sulfur, nitrogen, and phosphorous can be utilized as corrosion inhibitors when in acidic media. Adsorption of these compounds leads to a protective layer on the metal surface, which reduces corrosion rates and keeps corrosive elements away from the metal. However, these compounds are artificial and expensive and also harmful to both human and the green environment. Therefore, it should be supplanted with non-toxic and eco-friendly

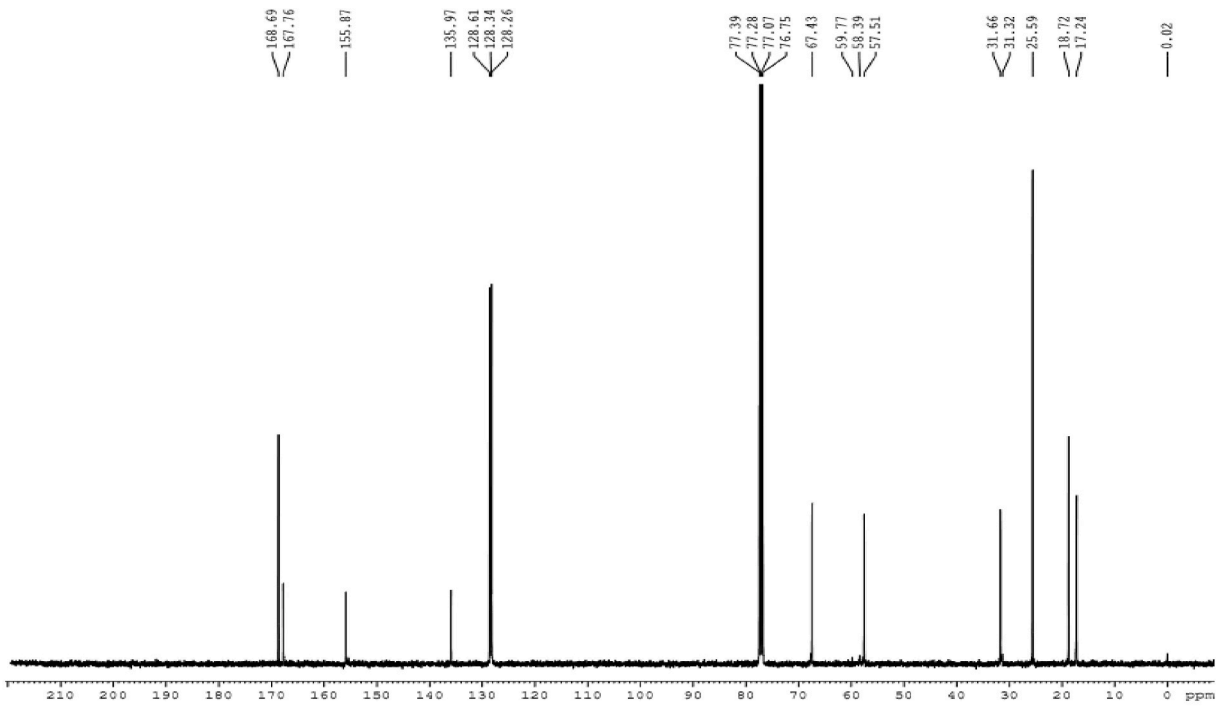

(a)

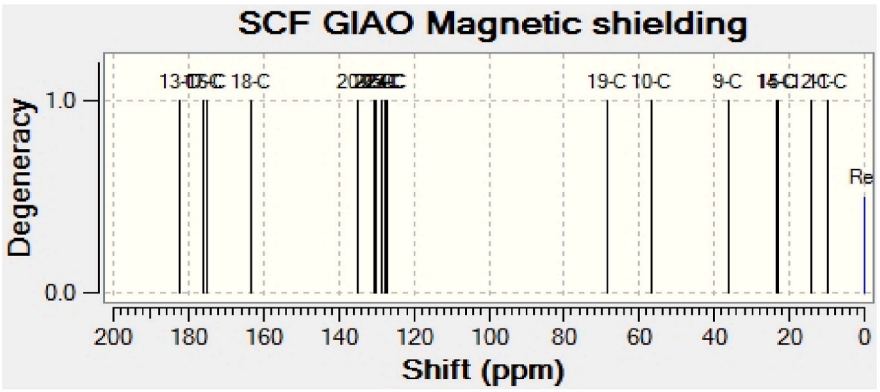

(b)

Fig. 6a. (a&b): Experimental and theoretical 13C NMR spectra of Carbobenzoxy L-Valine Succinimidyl Ester.

compounds [30].

Inhibitor performance was determined by a wide range of experimental techniques, but these are expensive and time-consuming to implement. Finding the active sites on a molecule is also a challenge [31]. In recent years, theoretical techniques including density functional theory (DFT) can help determine the molecular active sites and the inhibition efficiency of those active sites. Amino acids belongs to the class of non-toxic organic compounds, which are readily soluble in aqueous solutions, are eco-friendly and easy to manufacture at low cost [32].

Existence of heteroatoms (N, S, P and O) in any compound progresses its action as ferrous corrosion inhibitor. A sole pair of electrons is available on N and O-atoms, thus assisting creation of chemical bonds with the surface of metal atoms. CVSE contains both nitrogen and oxygen atoms on its structure. This favors the CVSE to act as a corrosion inhibitor.

With a support of global reactivity descriptor, the inhibition nature of CVSE was inspected. A molecule with high global softness will interact and adhere to a metal surface more readily. On the other hand molecule with lower η (and higher value of S) values show higher corrosion inhibition.

Energy gap (Eg) measures how reactive organic molecules are to metal surfaces (Fe) [33]. As the energy gap decreases, more organic molecules bind to a metal surface, and this results in an increase in adsorption onto the metal surface. It has been described that the binding ability of organic molecules to a metal surface can be characterized by energy gap in a number of literatures. A molecule with a low energy gap is more polarizable and has a high chemical reactivity and poor kinetic stability [34]. Comparatively, CVSE 1 (CVSE with thiophene donor; cyanoacrylic acceptor) has the least energy gap and exhibits good corrosion inhibition.

Among all the other compounds, CVSE 1 has the lowest value of η, therefore it has the highest inhibition efficiency. Equation (7) was used to compute the fraction of electrons transferred (ΔN) from the inhibitor molecule to the surface of Fe atoms. Depends upon the polarity (positive or negative) of ΔN, transferring of electron occurs from the inhibitor to the Fe surface and vice-versa [35]. Table 9 confirms that among all molecules, CVSE 1 has positive ΔN, thus specifying adsorption through electron donation by the CVSE molecules. Less negative $\Delta E_{back\text{-}donation}$

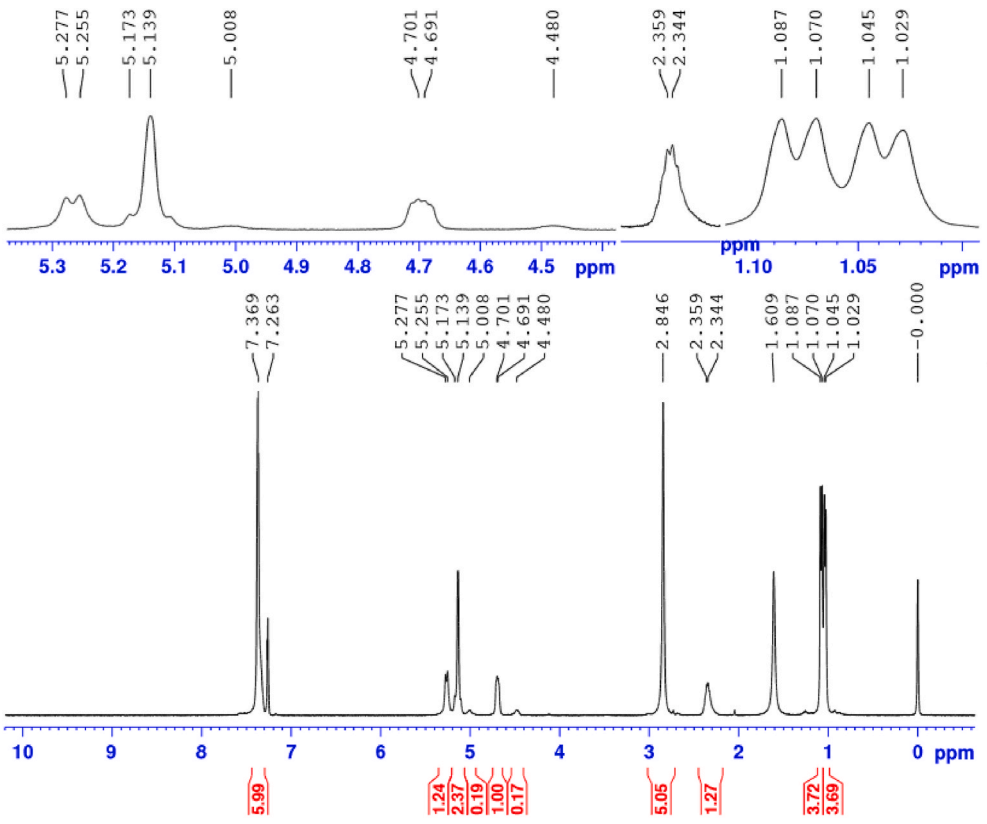

(a)

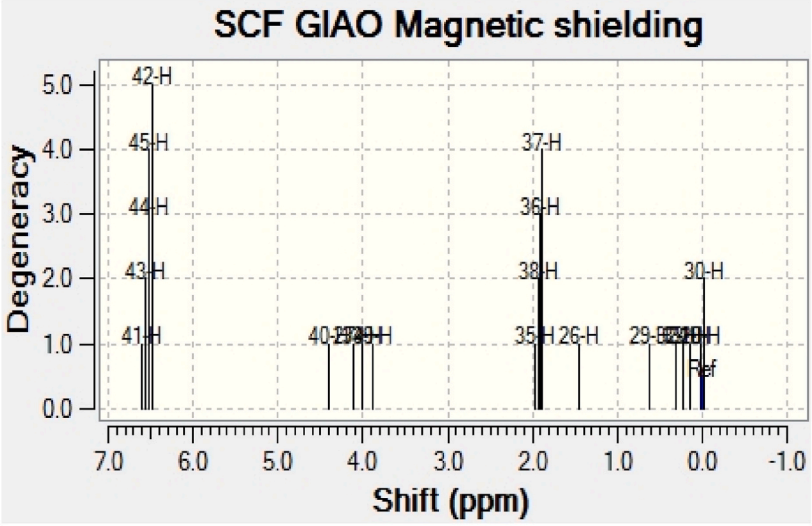

(b)

Fig. 6b. (b): Experimental and theoretical ^{1}H NMR spectra of Carbobenzoxy L-Valine Succinimidyl Ester.

offers better corrosion inhibiting efficiency. CVSE 1 has less negative $\Delta E_{back\text{-}donation}$ and representing its maximum inhibition effectiveness.

Using condensed Fukui functions indexes, one can determine the atoms in a molecule that are more likely to either donate electrons or accept electrons. It was suggested that N8 is believed to be a predominantly active region for reactions with metal (Fe) atoms.

5. Conclusion

Experimental and theoretical (using DFT B3LYP/6–311 G) evaluations were carried out on the title compound. The structure was optimized and the geometrical parameters were compared with the experimental results. The spectroscopic FTIR, NMR, and UV-Vis studies were carried out on CVSE and compared with the theoretical values The calculated HOMO-LUMO energies also shows that transferring of charge

Table 8a
The calculated[13]C, isotropic chemical shifts (all values in ppm) for *N*-Carbobenzoxy-L-Valine-Succinimidyl Esterusing DFT/B3LYP/6–311 G method.

Atoms	Experimental	Theoretical	
	Chemical shift	Chemical shift	Chemical shielding
C9	31.32	36.2632	146.2024
C10	57.51	56.7551	125.7105
C12	17.24	14.0009	168.4647
C13	–	182.5009	−0.0353
C14	25.59	23.2773	159.1883
C15	18.72	22.8342	159.6314
C16	–	174.969	7.4966
C17	168.69	176.274	6.1916
C18	167.76	163.1142	19.3514
C19	67.43	68.3673	114.0983
C20	135.97	134.8233	47.6423
C21	–	130.6578	51.8078
C22	–	130.2005	52.2651
C23	128.26	127.574	54.8916
C24	128.34	127.3638	55.1018
C25	128.61	128.4736	53.9920

Table 8b
The calculated [1]H NMR isotropic chemical shifts (all values in ppm) for *N*-Carbobenzoxy-L-Valine Succinimidyl Ester using DFT/B3LYP/6-311G method.

Atoms	Experimental	Theoretical	
	Chemical shift	Chemical shift	Chemical shielding
H26	2.344	1.4461	30.4360
H27	4.691	4.1176	27.7645
H28	0.000	0.0176	31.8645
H29	1.087	0.6215	31.2606
H31	1.029	0.1443	31.7378
H32	1.045	0.3139	31.5682
H33	1.070	0.2348	31.6473
H34	4.701	3.9992	27.8829
H35	2.359	1.9629	29.9192
H36	2.846	1.902	29.9801
H37	1.609	1.8788	30.0033
H38	4.480	1.9351	29.9470
H39	5.008	3.8836	27.9985
H40	5.139	4.4065	27.4756
H41	5.173	6.6045	25.2776
H42	5.255	6.4763	25.4058
H43	5.277	6.5602	25.3219
H44	7.263	6.5251	25.3570
H45	7.369	6.5221	25.3600

Table 9
Calculated values of E_{HOMO}, E_{LUMO}, Electronegativity (χ) and ΔN values for *N*-Carbobenzoxy-L-Valine Succinimidyl Ester with donor variations using DFT/B3LYP/6-311G method.

Systems	E_{HOMO} (eV)	**E_{LUMO}** (eV)	Energy gap (Eg) (eV)	χ (eV)	Ƞ (eV)	ΔN	$\Delta E_{back\text{-}donation}$
CVSE	−8.3096	−4.1021	4.2075	6.2059	2.1037	0.0432	−0.5259
CVSE1 Donor: Thiophene; Acceptor: Cyanoacrylic	**−7.0442**	−5.0254	**2.0188**	6.0348	1.0094	**0.1747**	**−0.2523**
CVSE2 Donor:Furan; Acceptor: Cyanoacrylic	−7.6997	−5.3088	2.3908	6.5042	1.1954	−0.0487	−0.2988
CVSE3 Donor: Pyrole; Acceptor: Cyanoacrylic	−7.9218	−5.0238	2.8979	6.4728	1.4489	−0.0293	−0.3622
CVSE4 Donor: Azulene; Acceptor: Cyanoacrylic	−7.8778	−5.5311	2.3466	6.7045	1.1733	−0.1349	−0.2933

occurs within the molecule. The first order hyperpolarizability has the value of 1.9686×10^{-30} esu, which confirms the nonlinear optical properties of CVSE. Reactive sites of the compound were identified by Fukui function analysis. A simulation of the molecular electrostatic potential revealed that the title compound has electrophilic and nucleophilic properties. The highest HOMO energy and ΔN values confirms the highest inhibition efficiency. Theoretically, this approach can predict a potential inhibitor from amino acids and also helpful in their

rational design and synthesis for corrosion inhibition application.

Declaration of competing interest

There is no conflict of interest.

Acknowledgement

We thank Cauvery College for Women (Autonomous), Tiruchirappalli, for providing instrument facility under the support of DST-FIST-Level 0 program (Ref. No. SR/FST/College-246/2015(c)).

References

[1] G. Wu, Amino Acids: Biochemistry and Nutrition, CRC Press, Boca Raton, 2013, https://doi.org/10.1201/b14661.
[2] T. Mallik, T. Kar, Synthesis, growth and characterization of a new nonlinear optical crystal: L-arginine maleate dehydrate, J. Cryst. Growth 04 (02) (2005) 143–153, https://doi.org/10.1002/crat.200410430.
[3] Corrosion inhibition of carbon steel in 1 M H2SO4 using new Azo Schiff compound: electrochemical, gravimetric, adsorption, surface and DFT studies, J. Mol. Liq. 315 (2020), 113690.
[4] M.S. Masoud, M.K. Awad, M.A. Shaker, El-Tahawy, The role of structural chemistry in the inhibitive performance of some aminopyrimidines on the corrosion of steel, Corrosion Sci. 52 (2010) 2387–2396, https://doi.org/10.1016/j.corsci.2010.04.011.
[5] D. Xu, M. Jiang, Z. Tan, A new phase matchable nonlinear optical crystal—L-arginine phosphate monohydrate (LAP), Acta Chem. Sin 41 (1983) 570, https://doi.org/10.1002/cjoc.19830010217.
[6] M.J. Frisch, G.W. Trucks, H.B. Schlegal, et al., GAUSSIAN 09, Revision A.02, Gaussian, Inc., Wallingford CT, 2009.
[7] N. Sundaraganesan, S. Kalaichelvan, C. Meganathan, D. Dominicm Joshua, J. Cornard, FT-IR, FT-Raman spectra and ab initio HF and DFT calculations of 4-N, N'-dimethylamino pyridine, Spectrochim. Acta, Part A 71 (2008) 898, https://doi.org/10.1016/j.saa.2008.02.016.
[8] C. Usha, R. Santhakumari, Lynnette Joseph, D. Sajan, R. Meenakshi, A. Sinthiya, Growth and combined experimental and quantum chemical study of glycyl, L-Valine crystal Heliyon 5 (2019), e01574, https://doi.org/10.1016/j.heliyon.2019.e01574.
[9] M. Amalanathan, I. Hubert Joe, V.K. Rastogi, Density functional theory calculations and vibrational spectral analysis of 3,5-(dinitrobenzoic acid), J. Mol. Struct. 985 (2011) 48–65, https://doi.org/10.1016/j.saa.2011.01.023.
[10] Sweta Moitra, Saikat Kumar Seth, Tanusree Kar, Synthesis, crystal structure, characterization and DFT studies of L-valine L-valinium hydrochloride, J. Cryst. Growth 312 (2010) 1977–1982, https://doi.org/10.1016/j.jcrysgro.2010.03.016.
[11] C. Charanya, S. Sampathkrishnan, N. Balamurugan, Quantum chemical computations, molecular docking, experimental and DFT calculation of 4-amino-3-phenylbutanoic acid, Polycycl. Aromat. Comp. (2020), https://doi.org/10.1080/10406638.2020.1776347. ISSN: 1040-6638 (Print) 1563-5333 (Online).
[12] V. Arjunan, et al., Synthesis, FTIR, FT-Raman, UV–visible, ab initio and DFT studies on benzohydrazide, Spectrochim. Acta, Part A 79 (2011) 486–496, https://doi.org/10.1016/j.saa.2011.03.018.
[13] M. Snehalatha, C. Ravikumar, I. Hubert Joe, V.S. Jayakumar, Vibrational spectra and scaled quantum chemical studies of the structure of Martius yellow sodium salt monohydrate, J. Raman Spectrosc. 40 (9) (2009) 1121–1126, https://doi.org/10.1002/jrs.2244.
[14] B. Smith, Infrared Spectral Interpretation, CRC Press, 1998, https://doi.org/10.1201/9780203750841.
[15] P. Hobza, Z. Havlas, Blue-shifting hydrogen bonds, Chem. Rev. 100 (2000) 4253–4264, https://doi.org/10.1021/cr990050q.
[16] Synthesis, Spectrophotometric and DFT studies of new triazole schiff bases as selective naked-eye sensors for acetate anion, Supramol. Chem. (2020), https://doi.org/10.1080/10610278.2020.1808217.
[17] R. Meenakshi, Spectral investigations, DFT based global reactivity descriptors, Inhibition efficiency and analysis of 5-chloro-2-nitroanisole as π-spacer with donor-acceptor variations effect for DSSCs performance, J. Mol. Struct. 1127 (2017) 694–707, https://doi.org/10.1016/j.molstruc.2016.08.030.
[18] T. Koopmans, Über die Zuordnung von Wellenfunktionen und Eigenwerten zu den Einzelnen Elektronen Eines Atoms, Physica (1934) 104–113, https://doi.org/10.1016/S0031-8914(34)90011-2.
[19] Ralph G. Pearson, Chemical Hardness: Applications from Molecules to Solids, Wiley-VCH, Weinheim, Germany, 1997, ISBN 978-3-527-60617-7.
[20] P.W. Ayers, R.G. Parr, Local hardness equalization: exploiting the ambiguity, J. Chem. Phys. 128 (2008), 184108, https://doi.org/10.1063/1.2918731.
[21] S. Kaya, et al., Determination of corrosion inhibition effects of amino acids: quantum chemical and molecular dynamic simulation study, J. Taiwan Inst. Chem. Eng. (2015) 1–8, https://doi.org/10.1016/j.jtice.2015.06.009.
[22] W. Yang, W.J. Mortier, The use of global and local molecular parameters for the analysis of the gas-phase basicity of amines, J. Am. Chem. Soc. 108 (19) (1986) 5708–5711, https://doi.org/10.1021/ja00279a008.
[23] C. Lee, W. Yang, R.G. Parr, José L. Gázquez, A hardness and softness theory of bond energies and chemical reactivity, Theol. and comp. Chem. 5 (1998) 135–152, https://doi.org/10.1016/S1380-7323(98)80007-1.
[24] K. Venil, A. Lakshmi, V. Balachandran, B. Narayana Vinutha, V. Salian, FT-IR and FT-Raman investigation, quantum chemical analysis and molecular docking studies of 5-(4-Propan-2-yl)benzylidene)- 2-[3-(4-chlorophenyl)-5[4-(propan-2-yl) phenyl-4,5-dihydro-1H-pyrazol-1-yl]-1,3-thiazol-4(5H)-one, J. Mol. Struct. 1225 (2021), 129070, https://doi.org/10.1016/j.molstruc.2020.129070.
[25] K. Sarojinidevi, P. Subramani, M. Jeeva, N. Sundaraganesan, M. Susai Boobalan, G. Venkatesa Prabhu, Synthesis, molecular structure, quantum chemical analysis, spectroscopic and molecular docking studies of N-(Morpholinomethyl) succinimide using DFT method, J. Mol. Struct. 1175 (2018), https://doi.org/10.1016/j.molstruc.2018.07.101.
[26] V. Arjunan, R. Santhanam, T. Rani, H. Rosi, S. Mohan, FTIR, FT-Raman, FT-NMR and quantum chemical investigations of 3-acetylcoumarin, Spectrochim. Acta Mol. Biomol. Spectrosc. 109 (2013) 79–89, https://doi.org/10.1016/j.saa.2013.01.100.
[27] K. Pihlaja, E. Kleinpeter (Eds.), Carbon-13 NMR Chemical Shifts in Structural and Sterochemical Analysis, VCH Publishers, Deerfield Beach, 1994. ISBN-10: 0895733323, -13:978-0895733320.
[28] B. Osmiałowski, E. Kolehmainen, R. Gawinecki, GIAO/DFT calculated chemical shifts of tautomeric species. 2-Phenacylpyridines and (Z)-2-(2-hydroxy-2-phenylvinyl)pyridines Wiley Ana, Science 39 (2001), https://doi.org/10.1002/mrc.856.
[29] C. Dariva, A. Galio, Corrosion inhibitors–principles, mechanisms and applications, in: Developments in Corrosion Protection, Intech Open, 2014, pp. 365–379, https://doi.org/10.5772/57255.
[30] M. Masoud, M. Awad, M. Shaker, M. El-Tahawy, The role of structural chemistry in the inhibitive performance of some aminopyrimidines on the corrosion of steel, Corrosion Sci. 52 (2010) 2387–2396, https://doi.org/10.1016/j.corsci.2010.04.011.
[31] J. Radilla, G. Negrón-Silva, M. Palomar-Pardavé, M. Romero-Romo, M. Galván, DFT study of the adsorption of the corrosion inhibitor 2-mercaptoimidazole onto Fe (100) surface, Electrochim. Acta 112 (2013) 577–586, https://doi.org/10.1016/j.electacta.2013.08.151.
[32] R. Loto, Corrosion inhibition effect of non-toxic α-amino acid compound on high carbon steel in low molar concentration of hydrochloric acid, J. Mater. Res. Technol. 8 (2019) 484–493, https://doi.org/10.1016/j.jmrt.2017.09.005.
[33] H. Nwankwo, L. Olasunkanmi, E. Ebenso, Experimental, quantum chemical and molecular dynamic simulations studies on the corrosion inhibition of mild steel by some carbazole derivatives, Sci. Rep. 7 (2017), https://doi.org/10.1038/s41598-017-02446-0.
[34] I.B. Obot, N.O. Obi-Egbedi, A.O. Eseola, Anticorrosion potential of 2-mesityl-1H-imidazo[4,5-f][1,10]phenanthroline on mild steel in sulfuric acid solution: experimental and theoretical study, Ind. Eng. Chem. Res. 50 (2011) 2098–2110, https://doi.org/10.1021/ie102034c.
[35] Dharmendr Kumara, Nimesh Jainb, Vinay Jaina, Beena Raia, Amino acids as copper corrosion inhibitors: a density functional theory approach, App. Sur. Sci. 514 (2020), 145905, https://doi.org/10.1016/j.apsusc.2020.145905.